Journal of Structural Engineering & Applied Mechanics (2023) 6(5):490-506
DOI 10.31462/jseam.2023.05490506

RESEARCH ARTICLE

Experimental investigation and numeric modelling of the impact performance of basalt fiber reinforced geopolymer concrete

Hiranur Güngör[1], Berivan Yılmazer Polat[1*]

[1] Munzur University, Faculty of Fine Arts, Design and Architecture, Tunceli, Turkiye

Article History

Received 20 September 2023
Accepted 25 December 2023

Keywords

Geopolymer concrete
Drop-weight impact test
Basalt fiber
SEM
Modelling

Abstract

Geopolymer concrete (GC) has been found to have better results than Portland cement concrete (PCC), including lower carbon dioxide emissions, higher compressive strength, and greater durability. The study aims to determine the effects of basalt fiber on GC due to the impact caused by the sudden loading effect. Samples were prepared with different mixing ratios for the experimental process, with PCC used as the control sample. Basalt fibers were added to the samples in three different ratios based on optimal mixing ratios determined through physical and mechanical tests, such as UPV (Ultrasonic Pulse Velocity), compressive strength, and flexural strength. Subsequently, fibrous samples were analyzed using SEM (scanning electron microscopy) and EDS (energy dispersive spectroscopy). A drop-weight experiment was conducted on GC plates measuring 50×50×5 cm, which contained two different fiber ratios that yielded the best mechanical and physical properties. The results were analyzed using numerical modeling methods. No changes in content were made. The sample with the highest impact resistance was found to be the 2% basalt fiber-reinforced GC, with a displacement value 21.21% lower than PCC. The language used is clear, concise, and objective, with a formal register and precise word choice. The text follows a logical structure with causal connections between statements and adheres to conventional academic formatting and citation styles. The ANSYS modeling results indicated an 89.63% similarity with the experimental data regarding the displacement values. Additionally, the study demonstrated that the inclusion of basalt fiber additives enhances the impact resistance of geopolymer concrete. Furthermore, numerical modeling can predict the impact behavior of concrete to a significant extent, eliminating the need for experimental processes.

1. Introduction

The most used building material today is conventional concrete. The concrete industry needs help in meeting the need for Portland cement concrete (PCC) due to the slow progress of production, the limited limestone reserves, and increased carbon emissions [1]. But now, due to society's global climate crisis, research has been conducted on alternative materials such as geopolymer concrete, in other words, cementless concrete. Geopolymer concretes (GC) have recently been used as an alternative to PCC. The main reason is that GC

* Corresponding author (bpolat@munzur.edu.tr)
eISSN 2630-5763

contains different binders instead of cement. Portland cement (PC) needs excess fuel and high-temperature furnaces during production. GC has created an environmentally friendly alternative to PCC [2].

The properties of GC can be optimised with the right selection of raw materials, the right mixing, and the processing design to suit a specific application. The most important factors affecting GC properties can be listed as the SiO_2/Al_2O_3 ratio, R_2O/Al_2O_3 ratio, SiO_2/R_2O ratio (R = Na or K), and the liquid-solid ratio. Depending on this list, NaOH and Na2SiO3 were used in this study to create an alkaline silica reaction. In addition, previous studies have reported that GC has high early strength, low shrinkage; freeze-thaw, sulphate, corrosion, and acid resistance; resistance to fire, high durability, and alkaline aggregate reaction [3].

It has been observed that GCs exhibit excellent volume stability and better durability compared to PCC Also, including different types of fibers in the geopolymer matrix has proven useful in achieving the desired mechanical and durability properties [4]. One of these is basalt fiber (BF). Because these fibers are obtained from volcanic rocks, BF's strength, durability, and temperature resistance are high [5]. BF production cost may be low [6]. In addition, BF fills the cracks that will form in the concrete and delays the crack expansion, allowing excessive amounts of energy to be absorbed. Thus, it increases the impact resistance of concrete [7]. An impact-resistant reinforced GC can be used in strategic structures to minimize the impact of sudden loads caused by rocket attacks on airport runway concretes, concrete roads, and security barriers [8]. Impact experiments are used to observe the impact resistance of concrete. Dynamic loads (i.e., impact) are often attractive for researchers to characterize the response of material subjected to such loads, especially in military applications. The damages caused by impact loads vary depending on the impact speed, load, geometry, and material properties of the structure [9].

Considering the difficulties and cost of working on large concrete slabs, the method of estimating the results through modelling is available in the literature. In his study, Madheswaran et. al. analysed the results using the finite element method (FEM) of reinforced geopolymer concrete slab with dimensions of 1×1 m and thickness of 60 mm and only supported boundary conditions [10]. When another study was examined, the results obtained by ANSYS software concluded that reinforced GC and standard PCC showed similar deviations [11]. In a research that has prepared hardened concrete beams with a size of 100×150×1000 mm under steam curing for 24 hours. Then it was left to ambient curing for up to 28 days. The beams were tested for the two-point load method, and deviations were measured. ANSYS models were created, and experimental results were compared with ANSYS models. The modelling results gave values close to experimental results [12].

Numerous studies on geopolymer concrete exist in the literature. However, studies about impact resistance and modeling of basalt fiber-reinforced geopolymer concrete (BFGC) formed because of falling weight experiments in real dimensions have yet to be encountered. Therefore, the data obtained from this study will provide new findings and contribute to the originality of the research. It is expected that this study will lead to further research in this area. The primary objective of this study was to determine the optimal mixing ratio of geopolymer concrete for slab samples subjected to impact experiments. To achieve this, ten different mixing ratios were tested, varying the percentage of mineral additives. The binder used in this study was blast furnace slag. Compressive and flexural tests were conducted on cube samples measuring 10×10×10 cm and beam samples measuring 10×10×50 cm, which were prepared using the determined mixing ratios and tested on the 28th day. Additionally, a test was conducted to measure the quality of the fresh concrete's fluidity. Then, the fibrous samples were poured using the mixing ratio that yielded the best results in the tests, namely BS10, and the same tests were applied to them. For the slab samples, fiber ratios of 1% and 2% were chosen as they produced better results than samples with basalt fiber added in a ratio of 0.5%-1%-2% by volume. The slabs were prepared using a %1 and %2 fiber ratio in the BS10 mixing ratio. A drop-weight

impact test was conducted on the samples, and the deformation data were compared with the ANSYS Package Program simulation. The inferences intended to be drawn from this study are:

- To observe the effect of BF on impact, compressive and flexural strength.
- To determine the ratio in which mineral additives perform better.
- Comparison of GC and PCC in terms of mechanical and impact resistance.
- Comparing the numerical analysis results with experimental data.

2. Experimental program

The experimental and numerical flowchart of the study is indicated in Fig.1.

2.1. Materials

The materials used to construct GC samples are aggregates, alkaline liquids, water, superplasticizer, and mineral additives. This study used ASTM-F to grade the fly ash (FA) with a low calcium content. Blast furnace slag (BFS) is generally preferred for increasing the strength and durability of concrete without thermal curing [13]. In this study, BFS was used as a binding material in GC. On the other hand, CEM II/42.5 cement was chosen as the control sample poured PCC because it contains limestone and slag in its construction and has a strength of 42.5+ MPa. Silica fume (SF) is used in concrete to improve its properties, such as compressive and adhesion strength; it reduces permeability [14]. The chemical properties of SF, BFS, and FA are indicated in Table 1.

As an alkaline activator, the Na_2SiO_3/NaOH ratio was 2.5. 12 M NaOH solution selected [15]. 0-5 mm fine aggregate and sand, 5-12 mm coarse aggregate were used, and the water was used only to saturate the aggregate. The value was determined according to the water absorption capacity of the aggregate. Another material used for GC is BF. Fiber reinforcement has been made to increase the flexural strength of GC [16]. In the study of Zhao and his colleagues, it was observed that the GC bond strength increases as the fiber length increases [17]. For these reasons and because using BF of different lengths is limited in the literature, 12-16 mm BF was preferred in this study. The fiber's physical and chemical properties are indicated in Table 2.

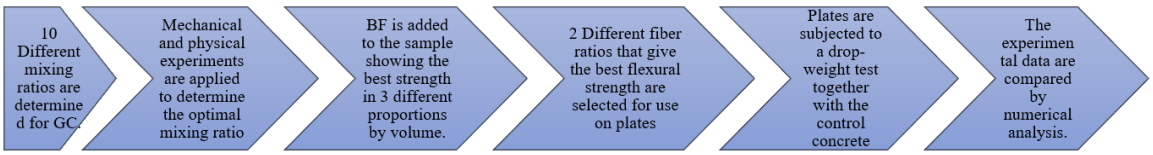

Fig. 1. Experimental and numerical flowchart

Table 1. The chemical properties of SF, BFS, FA

SF		BFS		FA	
Elements	Ratio	Elements	Ratio	Elements	Ratio
C_2O_3	3.5-5%	SO_3	0.20%	SO_3	0.20%
SiO_2	70-80%	MgO	59.37%	SiO_2	59.37%
Fe_2O_3	1.17-5.0%	S^{2-}	8.62%	Fe_2O_3	8.62%
Al_2O_3	2.55-4.10%	Cl	21.40%	Al_2O_3	21.40%
CaO	1.06-1.80%	CaO	32.55%	Cao	3.23%
MgO	8.05-9.9%	Si+Mg+Ca	2.10%	MgO	2.10%

Table 2. The physical and chemical properties of BF

Properties	Value	Module
Specific Gravity	2.60-2.80	g/cm^3
Length	12-16	mm
Diameter	9-23	μ
Tensile Strength	>4000	MPa
Elastic Modulus	80-90	GPa
Elongation at Break	2.0-4.5	%
Humidity	<1	%
Temperature of Application	-850	°C

The BF used in the experiment

This study used a superplasticiser that provides flowability/workability in polycarboxylic acid-based concrete. The superplasticizer was used in the proportion of 1% of the binder [18], and as a reinforcement, 15×15×0.5 cm (Q131/131) wire mesh steel is used.

2.2. Test samples and mixing proportions

The preliminary experimental samples consisted of a 10×10×50 mm beam and a 10×10×10 mm cube for each mixing ratio. Mechanical and physical experiments were conducted on these samples. A mixing ratio of 10 pieces was determined for the pre-test samples, as shown in Table 3. Due to the lack of a standard guideline, a trial-and-error procedure was adopted to determine the mixing ratio of the GCs.

The preliminary experiments determined the mixing ratio of the main experimental sample. Therefore, the BS10 mixing ratio, which provides the highest strength, was used (0.5%-1%-2%). The samples with added fiber were subjected to flowability, compressive, and flexural tests following the ASTM C1437 and ISO 9812 standards. [20,21]. The compressive strength test was performed on cubic samples with lengths of 10 cm by ASTM C39. The flexural strength was tested with a three-point flexural experiment on the 10×10×50 cm sized beam samples according to the TS EN 12390-5, ASTM C293M, and ASTM C923 standards [19,20]. Table 4 presents the detailed proportions of GC and PCC samples.

In a study, 200 mm flowability is defined as %100 flowability when the flowability of mortars is presented in mm [22]. When Table 5 is examined, the decrease in the BFS ratio with adding FA increased the workability. This is because when angular and flaky BFS particles are added to the rounded FA particles, it restricts the movement of the round FA particles, reducing the flow of the geopolymer paste. When the results were examined, it was found that PCC is less fluid compared to GC. A research was explained that this is due to the dense nature of the alkaline liquid used [23]. At last, the element that determines the choice between B100 and BS10 samples, which show similar values in terms of compressive strength, has been processed decisively. Therefore, the BS10 sample, which has relatively higher workability, was selected as the main mixing ratio. However, it has been observed that as the fiber ratio increases, the processability decreases. For this reason, fiber ratios such as 0,5%-1%- %2 were held at the border. To increase the fiber content, regardless of the type and geometry, reduces the flowability of fiber-reinforced geopolymer composites [24]. This supported by another study that increasing the fiber content, despite reducing the workability, leads to forming many microcracks instead of large macro cracks [25]. A mixing was prepared for PCC targeting an average workability value and PC52.5. The experiment compared the preliminary samples to determine the optimal ratio for propagation.

Table 3. Mixing ratios of 10 pieces determined for the pre-test samples

%	B100	BA10	BA20	BA30	BS10	BS20	BS30	BS50	S100	BSA25
SF	0	0	0	0	10	20	30	50	100	25
BFS	100	90	80	70	90	80	70	50	0	50
FA	0	10	20	30	0	0	0	0	0	25

Table 4. Mixing proportions for samples of GC and PCC (kg/m^3) [19]

Samples	Coarse Agg. (g)	Fine Agg.+Sand (g)	Binders (kg)			Alkaline Activator (g)		Fiber (g)	Water	Super-plas. (g)	L/B
	5-12 mm	0-5 mm	SF	BFS	PC	Na_2SiO_3	NaOH	Basalt			
BS10-F0.5	640	1180	40	360		114.3	45.7	1.35	0	4	0.4
BS10-F1	640	1180	40	360		114.3	45.7	2.7	0	4	0.4
BS10-F2	640	1180	40	360		114.3	45.7	5.4	0	4	0.4
PCC	800	920			550			0	198	0	0.36

Table 5. Flowability of samples

Samples	PCC	B100	BA10	BA20	BA30	BS10	BS20
Flowability (mm)	96	83	90	100	102	103	107
Samples	BS30	BS50	S100	BSA25	BS10-F0,5	BS10-F1	BS10-F2
Flowability (mm)	108	113	87	115	112	107	103

After considering all factors, we selected 1% and 2% fiber ratios for the impact tests. As a control sample, we prepared PCC plates sized 50×50×5 cm. In the drop-weight test, 50×50×5 cm-sized plates prepared with two different fiber ratios (1-2%) were used, which had better flexural strength when the preliminary experimental data were considered. In addition, a spherical-tipped impact hammer with a diameter of 9 cm and a weight of 3.035 kg was used. The experiment involved dropping a spherical impact hammer from a height of 4.13 m onto the middle point of the plates. The test method was applied based on the literature review due to the lack of standards for this experiment.

3. Numerical Analysis

3.1. Obtaining displacement data

This study uses the digital image processing method (DIPM). The reason is that installing data acquisition sensors in the material and device is a disadvantage in cost and time. Especially during the analysis of dynamic loads in structures, acceleration, speed, time, displacement, and data are important for damage detection. Slow motion video recording was captured with the help of a SONY RX 100-4 camera. The data were obtained by correlation-based template matching method. The pixel label in which the label is located is introduced to the software using the MATLAB language, and a displacement-time graph is taken [26].

3.2. Processing of displacement data to the program

Several material models are proposed and available in commercial software to describe the dynamic behavior of concrete. One of them is Riedel-Hiermaier-Thoma (RHT) model [27]. This study defined GC with RHT because it was thought to better describe concrete behavior under dynamic loads [28]. The literature took the RHT model used in the analysis [29]. Data on concrete with a compressive strength of 35 MPa is defined in the material library. The RHT model is formulated so that the entered data defines the compressive strength. Thus, the concrete defined in the library can be taken to select the material. The only factor that has changed has been the compressive and tensile strength depending on the concrete. Stainless steel has been selected for the dropped sphere. The density was entered as 7950 kg/m^3 to apply the sphere's weight. Fig. 2. shows the stages of modelling, meshing, and supporting the concrete, impact sphere, and wire steel.

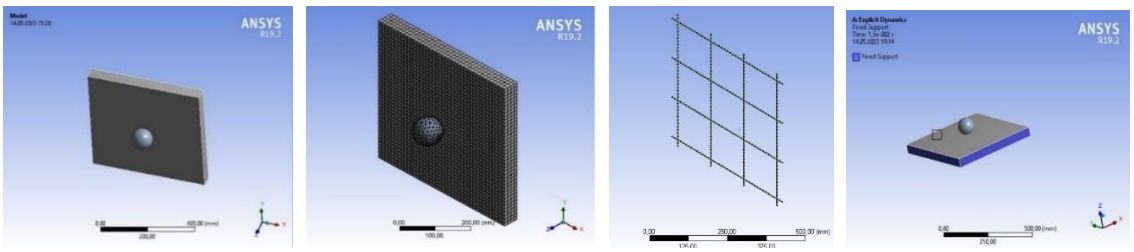

(a) (b) (c) (d)

Fig. 2. Concrete and impact sphere model (a), meshing(b), wire-steel meshing(c), supporting(d)

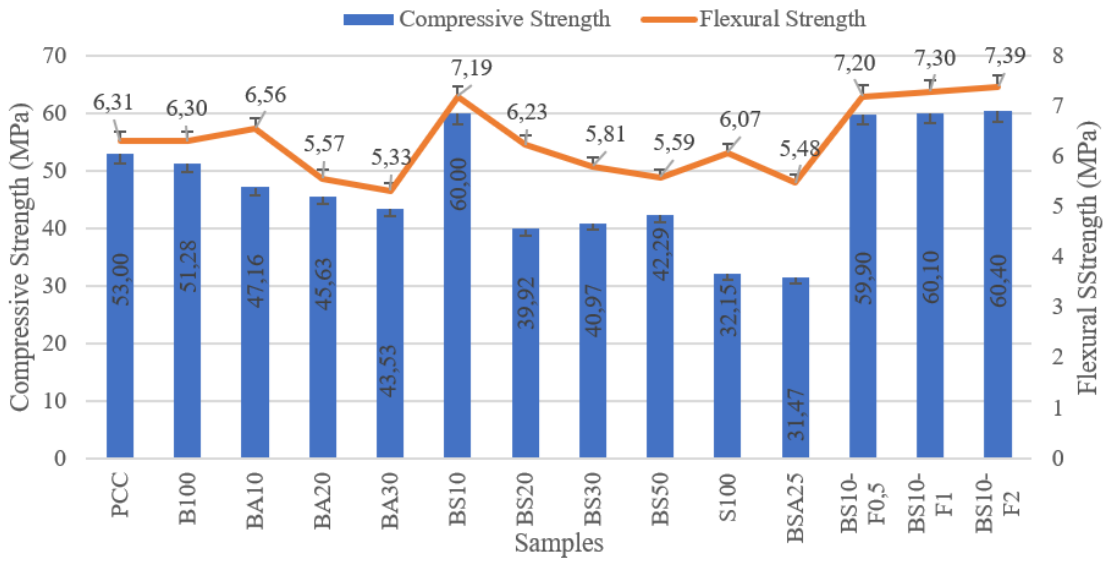

Fig. 3. Compressive and flexural strength of the 28th-day samples

4. Results and discussion

4.1. Compressive and flexural strength results

The formula below calculates the flexural strength of the concrete beam sections loaded from the middle.

$$R = 3\mathrm{PL}/2\mathrm{b}d^2 \quad (1)$$

where, R is the breaking modulus (MPa), P is the maximum load on the beam (N), L is the span length (mm), b is the average width of the beam cross section (mm), d is the average depth of the beam cross section (mm) [30].

The samples' maximum standard deviation ratio is 3%. As shown in Fig. 3, BS10, which yielded the highest strength of 60 MPa on the 28th day, was selected as the optimal mixing ratio. PCC is intended to produce a result similar to that of BS10, as it is a compressive strength control sample. Furthermore, the strength decreased with the addition of FA. In a reserch, the greatest compressive effect of FA was achieved by adding 50% to the mixture. The strength of the concrete decreases when it falls below 50%. Additionally, the flowability of the concrete increases with the addition of FA [31]. As a result, it can be inferred that the compressive strength decreased as the flowability increased. The strength of the mixture increased by 10% with the addition of SF. This can be attributed to the formation of a more compact structure by filling the voids with the microstructure of SF, thereby increasing the strength. . However, a decrease was observed in other ratios. UPV decreased as the SF participation rate increased. From here, it can be said that the concrete's strength decreases as its flowability increases when the SF ratio exceeds 10%. Just like in the FA, SF lost strength as the flowability of the concrete increased. However, when the SF contribution reached 100% on the 28th day, the strength decreased by 46.41%, 22.38%, 22% and 21.18%, respectively, compared to other SF ratios [32]. The reason for this may be the inability of the concrete to settle due to the low workability of the concrete. In the study of Singh et al., it was found that the strength decreased when SF was added to the mixing at a rate of 20% [31]. In addition, when Fig. 3 was examined, it was found that the fiber ratios changed by less than 1% and did not significantly affect compressive strength. To add BL by 1% has no significant effect on compressive strength [33]. However, in a study, it was concluded that the compressive strength of 2% BFGC is higher than 1% BFGC [34]. The literature shows parallels with the experimental results found. The flexural strength of 100% BFS-based GCs is 3.64% higher than 100% SF-based GCs [35]. This may be because SF increases the early-age strength of concrete[36]. As with the compressive strength on the 28th days, the flexural strength decreased as the SF ratio increased [36]. However, the flexural strength of 100% BFS-based GC is 3.64% higher than 100% SF-based GC. As with the compressive strength per day, the flexural strength decreased as the SF ratio increased. Like this result, Another research observed in their studies that the flexural strength decreases with increasing ratio in BFS-based GC, to which they added SF at a rate of 10% to 60% [37]. However, the flexural strength decreased when more than 10% FA was added to the BFS mixing. Similar results have been obtained in the literature [38]. Thus, it can be argued that adding FA and SF with small micron structures to more than 10% concrete yields poor results. It has shown values close to BS20 and BA20 because it has FA and SF at 25% of the BSA25 content. On the other hand, the PCC is similar to the literature; ANSYS Workbench software developed based on the FEM was used to compare the multiplication experiment results. Has shown values approximately close to B100 [19,36]. BS10 gave the highest result compared to other SF and mixing ratios. A study that the addition of SF at a rate of 10% is optimal [40]. The flexural strength values of fibrous GC were higher compared to non-fibrous mixings and PCC. Another a research has obtained similar results in his study [41]. Considering the experimental data obtained and the literature studies supporting them, the highest flexural strength was found when SF was added to the BFS mixing at 10%. In addition, since 1% BFGC and 2% BFGC have a higher flexural

resistance of 1.34% and 2.58% compared to 0.5% BFGC, respectively, these two fiber ratios were preferred for the main experiments.

The flexural and compressive strength correlation graphs are shown in Fig. 4. Considering the coefficient of determination (R2), it can be said that there is a strong correlation between flexural and compressive strength. This is because the coefficient of determination expresses how much of the change in the dependent variable is explained by the independent variable(s). This situation indicates the explanatory power of the regression model [38]. Besides, as seen in Fig. 5., the flexural and compressive strength increased linearly with the percentage increase of BF participating in the optimal mixing. It has also been observed in the literature that BF increases flexural strength [16]. As a result, the addition of fiber increases compressive and flexural strength.

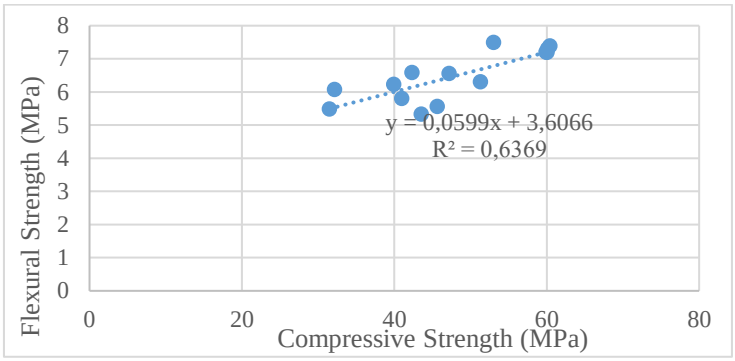

Fig. 4. Correlation between flexural and compressive strength

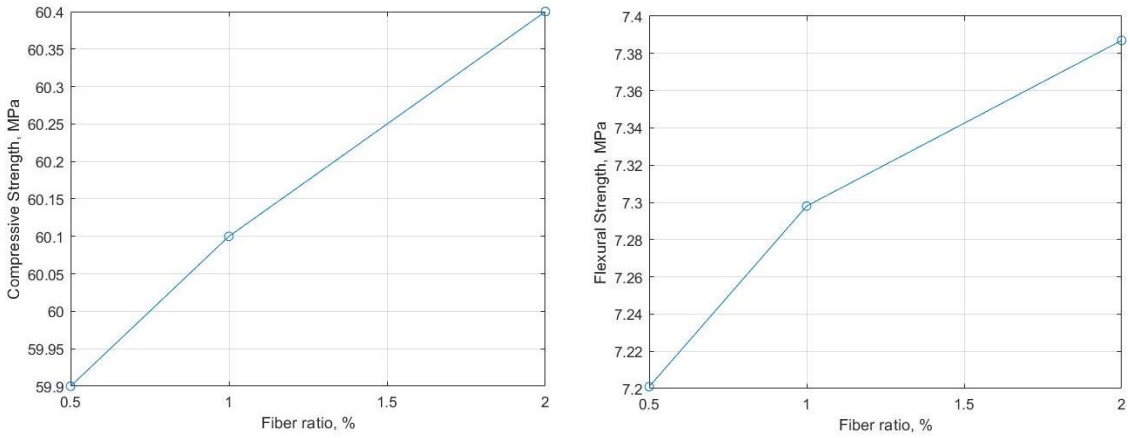

(a) (b)

Fig. 5. Correlation between fiber ratios and compressive (a) and flexural (b) strength

4.2. Ultrasound pulse velocity results

Ultrasonic pulse velocity (UPV) has been tested to measure the permeability of samples. Data were obtained with the help of sound waves based on ASTM C 597 [39]. The UPV is mainly related to the mixing density and the modulus of elasticity [41]. Accordingly, to reduce the separation rate, it is important that the concrete pouring is good and that enough thin material is used. In the experiment, good transition times with a sensitivity of 0.1 μ*s* were measured with an ultrasound instrument. The sound transition velocity was obtained by dividing the measured sample length by the recorded transition time[39]. The formula is given below:

$$V_s = \mathrm{l/t} \tag{2}$$

where, V_s is ultrasonic pulse velocity (km/s), l is transfer distance of electronic waves (mm), and t is ultrasonic pass rate (μs).

The max standard deviation ratio of the samples is 2%. In general, UPV represents the homogeneity and presence of defects in the microstructure and pore structure, such as voids and cracks, which directly affect the permeability properties of concrete [41]. When Fig. 6 was examined, as the FA ratio increased, the pass rate also increased. This is because the FA fills in the gaps and has a smaller micron size than the BFS. The fact that GC samples with FA added are more void-free than SF samples depends on their higher density [42]. When using 100% BFS, the sample's transition speed increases by 16.09% compared to the sample using 100% SF. The compressive strength of the B100 sample is 59.5% higher than that of the S100 sample, and its flexural strength is 3.78% higher. The UPV values are parallel to the compressive and flexural strengths. The BSA25 sample, which uses 25% FA and 25% SF, shows a 10.85% and 6.28% decrease in transition speed compared to concrete with 20% FA and 20% SF addition, respectively. The UPV values of the fibrous samples were the only ones that remained below 4000 m/s, possibly due to gaps created by the dispersion of fibers in the concrete. The figure shows that all the concrete samples have UPV values ranging from 3702 to 5228 m/s. According to the evaluation criteria specified in the Indian standards, it has been concluded that the concrete matrix contains very few gaps and cracks, is highly durable, and falls into the 'GOOD' and 'EXCELLENT' categories. [43].

4.3. SEM and EDS analyses

Scanning electron microscopy (SEM) and energy dispersive spectrometry (EDS) can be used as non-destructive methods to study the microstructure of materials. For instance, SEM and EDS can clarify the mechanism of strength development in hardened concrete samples by assessing porosity in their internal structure. [44]. The samples were prepared for the experiment according to the specified principles [45]. To comprehend the presence of fiber in samples with varying proportions of BF, we captured an SEM image of BF. For impact experiments, we used samples prepared with BF ratios of 1% and 2%. SEM and EDS analyses confirmed the presence of BF within the concrete.

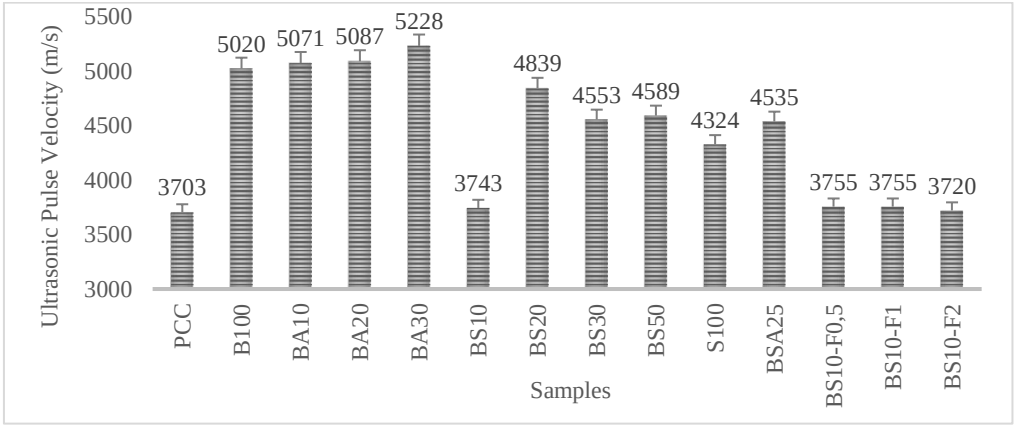

Fig. 6. UPV results of the samples

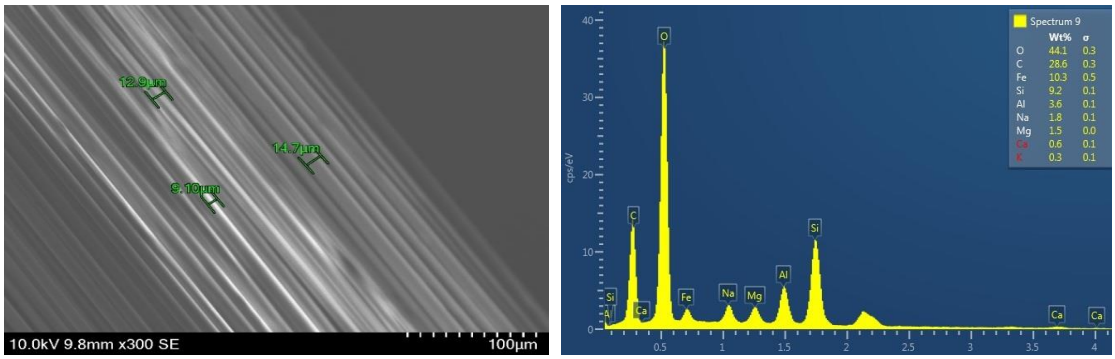

(a) (b)

Fig. 7. SEM image (a) and EDS result (b) of BF

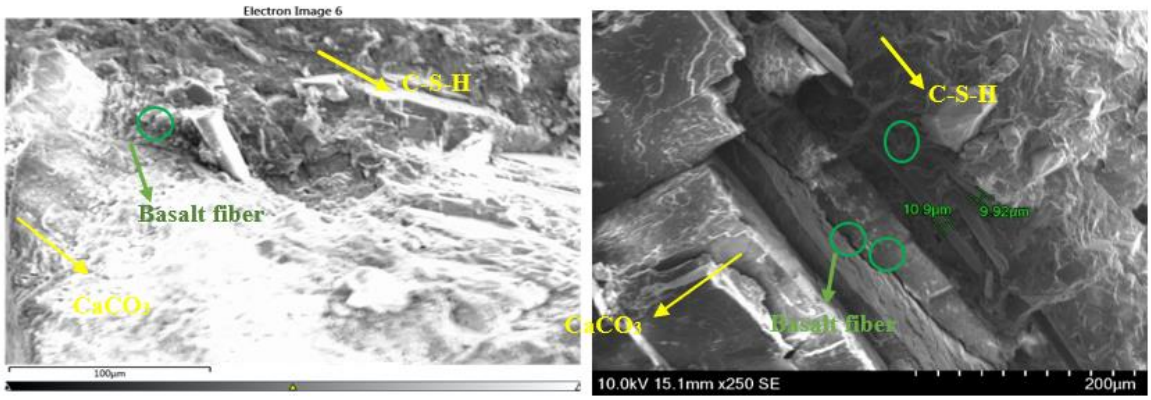

(a) (b)

Fig. 8. SEM images of (a) 1% and (b) 2% BFGC

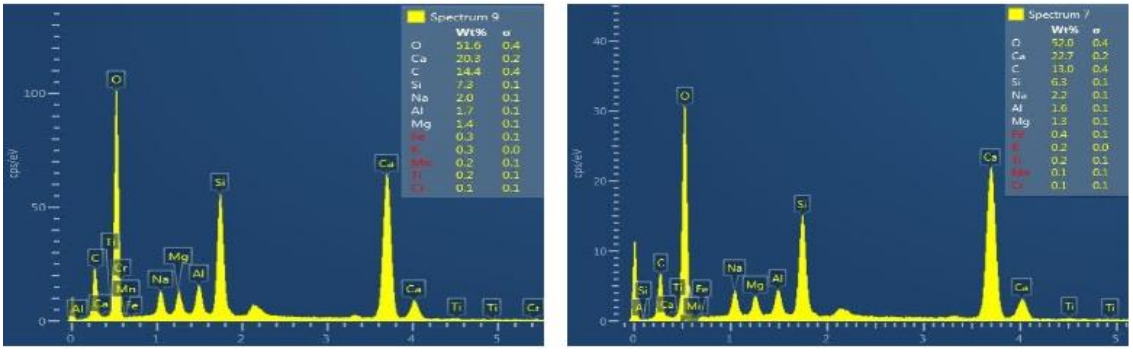

(a) (b)

Fig. 9. EDS results of 1% (a) and 2% (b) BFGC

Fig. 7 displays the internal structure of BF. SEM and EDS analyses provide an explanation for the presence of fibers in concrete and the elements that are present with the fibers. Upon initial examination of the EDS spectrum of BF, it is observed that it contains the following elements: O, C, Fe, Si, Al, Na, Mg, Ca, and K.

Fig. 8 displays the internal structures of samples with varying fiber ratios. The SEM images of GC samples aimed to prove the existence of BF and $CaCO_3$ and C-S-H gels resulting from geopolymerization.

The regions enclosed by green circles indicate basalt fiber. As can be seen from the SEM images, while one fiber was observed in the 1% fiber sample in Fig. 9a, three fiber contents were detected in the sample with 2% fiber content (Fig. 9b). The images demonstrate that the fibers are evenly distributed and not clumped, confirming the accuracy of the fiber ratios. The images demonstrate that the fibers are evenly distributed and not clumped, confirming the accuracy of the fiber ratios. Additionally, the microscope images reveal the presence of relatively harder structures, identified as $CaCO_3$, and gel-shaped structures, identified as C-S-H. [46].

In comparison, if elements observed in the content of BF are found in GC with different fiber content or if an increase in the percentage value of the element by weight is observed, it can be said that concretes contain BF. As shown in Fig. 9., the presence of the same element contents was preserved, and an increase in percentage values was detected. In addition, the formation of Mn, Ti, and Cr elements has been observed. Different element formations can explain this due to the reaction of BF with different structures in the concrete matrix by alkaline diffusion [47]. The GC matrix has the content of mineral additives and alkaline activators.

4.4. Drop-Weight impact test results

Fig. 10 shows the crack patterns and deformation occurring on the front and rear surfaces of 1%-2% BFGC and PCC samples after impact. Fig. 11. shows the experimental displacement-time graphs of the samples.

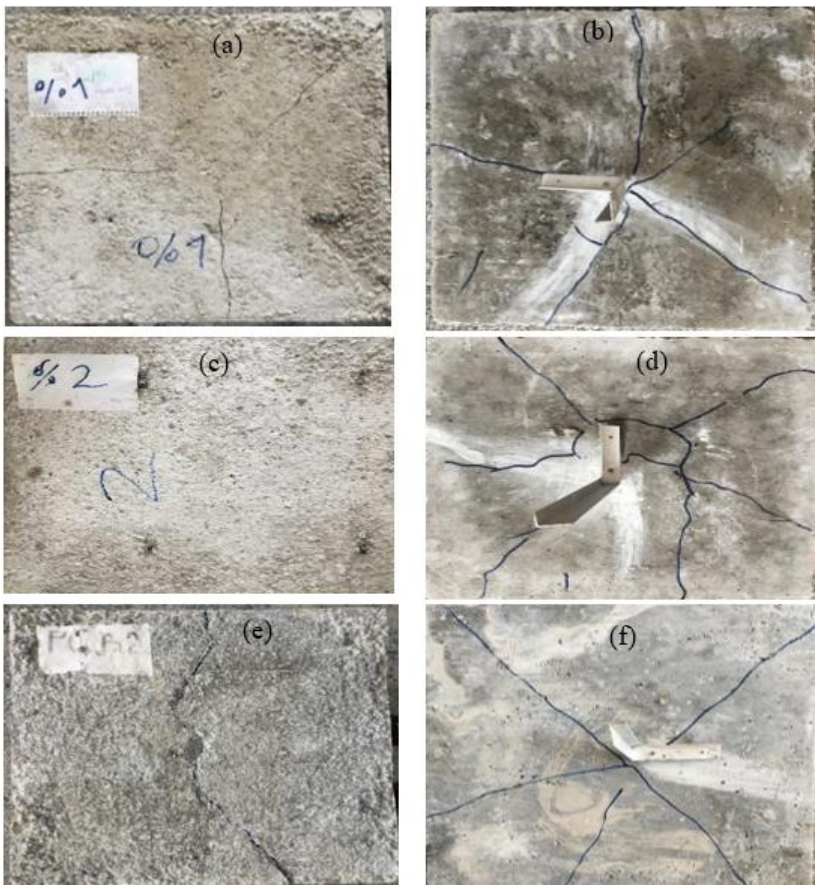

Fig. 10. Deformation occurring on the front (a), (c), (e) and rear (b), (d), (f) surface of respectively 1%-2% BFGC and PCC after impact blow

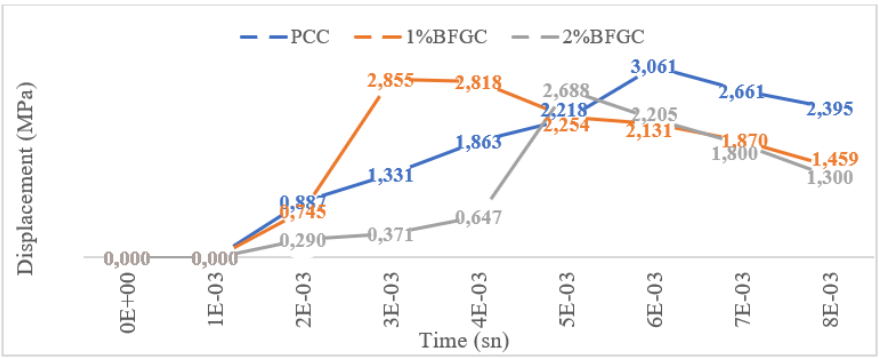

Fig. 11. Experimental displacement-time graph of samples

Table 6. Experimental displacement values of samples

Samples	Displacement (mm)
1% BFGC	2.78
2% BFGC	2.71
PCC	3.00

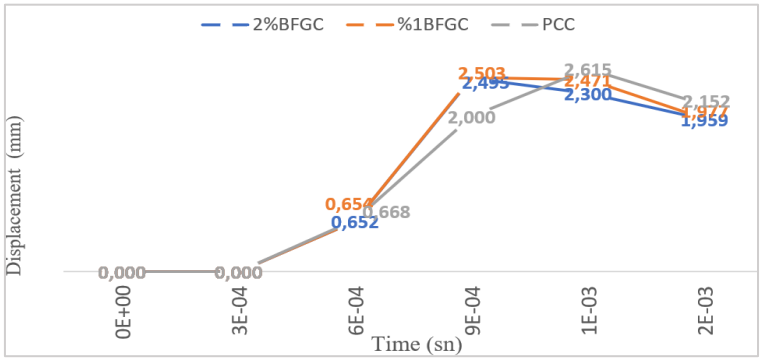

Fig. 12. Numerical displacement-time graph of samples

When Table 6 was examined, the largest displacement was observed in PCC samples with an average of 3.00 mm, while a smaller displacement of about 9.67% was detected in 2% BFGC. The presence and amount of fiber can explain this. Because as the fiber ratio increases, the flexural strength of the samples increases. The 2% BFGC, the highest sample with a flexural strength of 7.39 MPa, gave the least displacement value here, with an average of 2.71 mm. From here, it can be concluded that the BF has a healing effect on the displacements caused by sudden loads. In his study on two-way reinforced concrete, A previous research observed displacement values between approximately 2 and 3 mm on 100×100×7 cm sized plates of different fiber ratios due to a 7 kg spherical weight dropped from a height of 2.4 m. When a comparison was made according to these results, the displacement values found in this experimental study due to a weight of 3.035 kg from a height of 4.13 m to 500×500×50 cm plates gave approximate results. That is examined, it is expected that the displacement will increase as the drop height increases [48]. In the same way, Another research reported in their study that the displacement decreased with increasing plate thickness due to a drop-weight experiment they performed on sandwich plates with a size of 80×80×15 cm [49]. As a result of the drop-weight test performed on steel fibre-refiber-reinforce sandwich plates, they found a decrease in the maximum deviation of the plates due to the flexural stiffness of increasing plate thickness and increasing

load-bearing capacity [50]. Considering these studies, it can be said that BFGC gives better results than two-way reinforced concrete elements under load, which is loaded 23.77% faster on samples prepared in sizes smaller than the plate sizes used in Ref. 48. In parallel with this experimental study result, found that geopolymer concrete performed better under high-speed loads compared to PCC in their studies [51].

4.5. SEM and EDS analyses

This section of the study simulates the displacement of the concrete after the initial impact using ANSYS Workbench software. The drop-weight impact test results were compared with the Ansys workbench software developed using the finite element method. The multiplication simulation is modeled with Explicit Dynamics in ANSYS Workbench. This analysis was chosen because it can better analyze the material's structure under complex dynamic loads, such as impact [52]. Fig. 12. shows the numerical displacement-time graphs of the samples.

The analysis revealed that the displacement formed on 1% BFGC is approximately 2.50 mm, while the experimental data recorded a value of 2.78 mm. This indicates a decrease of 10% compared to the experimental data. The disparity observed may be attributed to the experimental conditions. To ensure one-to-one results, the input data for analysis needs to be at an appropriate level. The displacement caused by 2% BFGC is approximately 2.49 mm, whereas in the experimental data, this value was measured as 2.71 mm. Based on this, it was concluded that the analysis result exhibited an 8.11% decrease compared to the experimental data. The discrepancy may be attributed to the experimental conditions. The analysis input data should be refined to yield one-to-one results. The change in differences by 1.96% compared to 1% BFGC may also be dependent on experimental conditions. The experimental data showed a decrease of 2.51% and a displacement of approximately 2.61 mm on the PCC. This value was measured as 3.00 mm in the experimental data. It was determined that the analysis results showed a 13% decrease based on experimental data. Fig. 13 shows the samples' elastic strain and stress modes.

When Table 8 examined, the displacement of PCC is 8.49% higher than fibrous GC. This is because fiber-added concretes increase strength [54]. Since impact resistance is directly related to flexural strength, samples with higher flexural strength give higher impact resistance. According to the experimental results, fibrous concretes showed the highest flexural strength, averaging 7.295 MPa. It has been reported in the literature that fiber-doped concretes increase strength [54]. On the other hand, 2% BFGC showed 2.58% better displacement resistance compared to 1%BFGC. This may be because 2% BFGC has a 1.21% higher flexural strength than 1% BFGC. Finally, the displacement values formed from the analysis performed using FEM, like the literature, gave a result close to the experimental values of 89.63%. Khan et al. investigated the behavior of glass fiber concretes and reinforced concrete structures wrapped with BFs under impact. They have made comparisons by simulating experimental data with ANSYS. As a result, the experimental data gave overlapping results with the simulation [29,48].

From the study, it was concluded that finite element analysis is one of the best tools that can be used to determine the behavior of concretes under impact load accurately. The deformation that occurs during the design phase leads to experimental studies. Analysing the structural element designed with FEM saves cost and time during the experimental stage.

Table 7. Numerical displacement values of samples

Samples	Displacement (mm)
1% BFGC	2.50
2% BFGC	2.49
PCC	2.61

Table 8. Deviation of experimental and numerical displacement values

	Displacement (mm)		
Samples	Experimental	Numerical	Deviation (%)
1% BFGC	2.78	2.50	10.1
2% BFGC	2.71	2.495	8.0
PCC	3.00	2.61	13.0

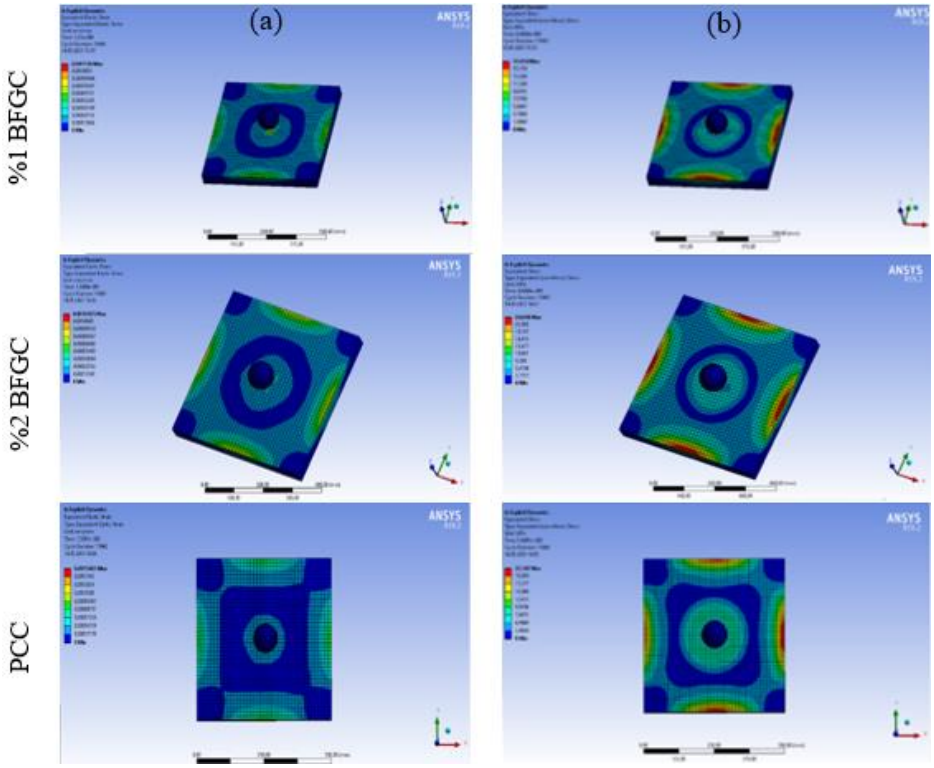

Fig. 13. Elastic strain (a) and stress (b) of the samples

5. Conclusions

The study investigated the impact behavior of geopolymer concrete with and without basalt fiber, analyzing the chemical and physical properties of the concrete and its response to impact. The results are presented below.

- By adding 10% SF to the GC, the highest compressive strength with 60 MPa and the highest flexural strength value with 7.19 MPa compared to other mixing ratios were found.
- By adding 10% SF to the GC, the compressive strength increased to 60 MPa, and the flexural strength value increased to 7.19 MPa, which were the highest values compared to other mixing ratios.
- The fibrous geopolymer concretes and PCC showed no significant difference in UPV results.
- GCs exhibited higher compressive strength than PCC, with an increase of 13.01% in 0.5% BF additive, 13.39% in 1% BF additive, and approximately 14% in 2% BL additive.
- The results show that GCs have higher flexural strength than PCC, with an increase of 14.15% at 0.5% BF additive, 14.58% at 1% BF additive, and 17.10% at 2% BF additive.

- The sample with the highest impact resistance was 2% BFGC due to the drop-weight test, with a displacement depth 6.06% lower than 1% BFGC and 21.21% lower than PCC.
- The ANSYS modelling data showed a 89.63% similarity to the experimental data obtained.

Based on these results, the test technique applied in the referenced study may provide more relevant results for making comparisons in academic studies to be conducted due to the lack of a specific test technique for the multiplication effect. Additionally, the strength of geopolymer concrete reinforcements can be strengthened by impact-damping materials.

Acknowledgments

This study was financially supported by the Scientific Research Projects Unit of Munzur University (MUBAP), project number YLMUB021_09. Additionally, Cenal Elektrik, Antalya Eti Krom, Mersin Oyak Cement, and Kompozit Pazarı provided mineral additives at no cost. Dr. Sedat Savaş and Ph.D. Student Mevlüt Emre Orhan helped to support us. We want to thank all of them sincerely.

Conflict of interests

The author(s) declared no potential conflicts of interest with respect to the research, authorship, and/or publication of this article.

Funding

This research received no external funding.

Data availability statement

No new data were created or analyzed in this study.

References

[1] Singh B, Ishwarya G, Gupta M, Bhattacharyya SK (2015) Geopolymer concrete: A review of some recent developments. Construction and Building Materials 85:78–90.

[2] Hasanbeigi A, Menke C, Price L (2010) The CO2 abatement cost curve for the Thailand cement industry. Journal of Cleaner Production 8(15): 1509–1518.

[3] Živica V, Palou MT, Križma M (2015) Geopolymer cements and their properties: A review. Building Research Journal 61(2):85–100.

[4] Mishra J, Panigrahi R (2020) Mini-Review on structural performance of fiber reinforced geopolymer concrete. International Journal of Innovative Technology and Interdisciplinary Sciences 3(2):435–442.

[5] Yalghuz MR (2020) Farklı Tip Malzemeler Kullanılarak Geopolimer Harç Üretimi ve Dayanıklılığının Incelenmesi. MSc Thesis. Eskişehir Technical University (in Turkish).

[6] Militký J, Kovačič V, Rubnerová J (2002) Influence of thermal treatment on tensile failure of basalt fibers. Engineering Fracture Mechanics 69(9):1025–1033.

[7] Hong GH and Shin YS (2003) Structural performance evaluation of reinforced concrete beams with externally bonded FRP sheets. Journal of the Korea Concrete Institute 15(1): 78–86.

[8] Di Ludovico M, Prota A, Manfredi G (2010) Structural upgrade using basalt fibers for concrete confinement. Journal of Composites for Construction 14(5): 541–552.

[9] Zhang MH, Shim VPW, Lu G, Chew CW (2005) Resistance of high-strength concrete to projectile impact. International Journal of Impact Engineering 31(7): 825–841.

[10] Madheswaran CK, Dattatreya JK, Ambily S (2020) Investigation on behaviour of reinforced geopolymer concrete slab under repeated low velocity impact loading. In International Journal of Innovative Research in Science, Engineering and Technology 3(3): 10775–10786.

[11] Kumar BSC and Ramesh K (2018) Analytical study on flexural behaviour of reinforced geopolymer concrete beams by ANSYS. In: Proceedings of IOP Conference Series: Materials Science and Engineering. Telangana, India.
[12] Aleem A, Arumairaj PD (2016) Analytical modeling of geopolymer concrete with manufactured sand using Ansys. International Journal of Advanced Engineering Technology VII (I):1253–1255.
[13] Sakulich AR (2011) Reinforced geopolymer composites for enhanced material greenness and durability. Sustainable Cities and Society 1(4): 195–210.
[14] Polat BY (2019) The investigation of self-healing of geoplymer mortar by using microorganisms. PhD Thesis, İstanbul Cerrahpaşa University.
[15] Kocabeyoğlu ET (2016) High temperature resistance of high strength mortars containing basalt fiber. Master's Thesis. Bozok University.
[16] Zhao J, Wang S, Wang Z, Wang K (2022) Experimental investigation on bond behavior of basalt fiber reinforced polymer bars to geopolymer concrete. Journal of Building Structures 43(6):245–256.
[17] Al-Majidi M, Lampropoulos A, Cundy AB, Meikle S (2016) Development of geopolymer mortar under ambient temperature for in situ applications. Construction and Building Materials 120:198–211.
[18] Nath P, Sarker PK (2017) Fracture properties of GGBFS-blended fly ash geopolymer concrete cured in ambient temperature. Materials and Structures. 50(1):1–12.
[19] ASTMC1437-07 (2008) Standard Test Method for Flow of Hydraulic Cement Mortar. Available at https://www.astm.org/c1437-20.html.
[20] ASTM C923/C293M (2002) Standard Test Method for Flexural Strength Concrete using Simple Beam with Center-Point Loading. Available at https://normanray.files.wordpress.com/2010/10/kuliah-7-c293.pdf.
[21] İpek S, Mermerdaş K (2022) Engineering properties and SEM analysis of eco-friendly geopolymer mortar produced with crumb rubber. Journal of Sustainable Construction Materials and Technologies 7(2): 95–107.
[22] Alexander AE, Shashikala AP (2022) Studies on the microstructure and durability characteristics of ambient cured FA-GGBS based geopolymer mortar. Construction and Building Materials 347:128538.
[23] Ranjbar N, Talebian S, Mehrali M, Kuenzel C, Cornelis Metselaar HS, Jumaat MZ (2016) Mechanisms of interfacial bond in steel and polypropylene fiber reinforced geopolymer composites. Composites Science and Technology 122:73–81.
[24] Ranjbar N, Zhang M (2020) Fiber-reinforced geopolymer composites: A review. Cement and Concrete Composites 17:103498.
[25] Erdoğan YS (2018) Computer vision based vibrational displacement measurement and modal identification. Dokuz Eylul University Eng. J. Sci. Eng. 20(59):201–211.
[26] Orhan ME (2021) Investigation of out-of-plane behavior of infill walls. MSc Thesis, Fırat University.
[27] Borrvall T, Riedel W (2011) The RHT concrete model in LS-DYNA. In: Proceedings of 8th European LS-DYNA conference. Strasbourg, France
[28] Pavlovic A, Fragassa C, Disic A (2017) Comparative numerical and experimental study of projectile impact on reinforced concrete. Composites Part B: Engineering 108:122–130.
[29] Vacev T, Zorić A, Grdić D, Ristić N, Grdić Z, Milić M (2023) Experimental and numerical analysis of impact strength of concrete slabs. Periodica Polytechnica Civil Engineering 67(1):325–335.
[30] Mbumbia L, de Wilmars AM, Tirlocq J(2000) Performance characteristics of lateritic soil bricks fired at low temperatures: a case study of Cameroon. Construction and Building Materials 14:(3): 121-131.
[31] Singh RP, Vanapalli KR, Cheela VRS, Peddireddy SR, Sharma HB, Mohanty B (2023) Fly ash, GGBS, and silica fume based geopolymer concrete with recycled aggregates: Properties and environmental impacts. Construction and Building Materials 378:131168.
[32] Sai DW, Satya ESRK (2019) Study on the mechanical properties of GGBS based geopolymer concrete using silica fume as a partial replacement. Journal on Structural Engineering 8(3):29.
[33] Dias DP, Thaumaturgo C (2005) Fracture toughness of geopolymeric concretes reinforced with basalt fibers. Cement and Concrete Composites 27(1):49–54.
[34] Ronad A, Karikatti VB, Dyavanal SS (2016) A study on mechanical properties of geopolymer concrete reinforced with basalt fiber. IJRET: International Journal of Research in Engineering and Technology 5(7):474–478.

[35] Gupta A, Gupta N, Saxena KK (2021) Mechanical and durability characteristics assessment of geopolymer composite (gpc) at varying silica fume content. Journal of Composites Science 5(9):237.
[36] Mustakim SM, Das SK, Mishra J, Aftab A, Alomayri TS, Assaedi HS, Kaze CR (2021) Improvement in fresh, mechanical and microstructural properties of fly ash- blast furnace slag based geopolymer concrete by addition of nano and micro silica. Silicon 13(8):2415–2428.
[37] Basheer B, Antherjanam G (2020) Effect of silica fume in the mechanical properties of ambient cured ggbs based geopolymer concrete. In: Proceedings of SECON'19: Structural Engineering and Construction Management 3 Springer International Publishing.
[38] Şahin MG (2017) Korelasyon ve Regresyon. In: Psikoloji için İstatistiksel Metotlar. pp. 251–302. Pegem Akademy (in Turkish).
[39] ASTM C597 (2016) Standard Test Method for Pulse Velocity Through Concrete. American Society for Testing and Materials. West Conshohocken, PA, USA.
[40] Cheah CB, Samsudin MH, Ramli M, Part WK, Tan LE (2017) The use of high calcium wood ash in the preparation of ground granulated blast furnace slag and pulverized fly ash geopolymers: A complete microstructural and mechanical characterization. Journal of Cleaner Production 156:114–123.
[41] Yap SP, Alengaram UJ, Jumaat MZ (2013) Enhancement of mechanical properties in polypropylene- and nylon-fibre reinforced oil palm shell concrete. Materials & Design 49:1034–1041.
[42] T. C. Holland (2005) Silica Fume User's Manual. TC Holland Technical Rep. No: FHWA IF, 5:9–10.
[43] IS 13311 (Part 1) (1992) Method of Non-destructive testing of concrete: Part 1: Ultrasonic pulse velocity. Bur. Indian Satandards 1:1–14.
[44] Ryu GS, Lee YB, Koh KT, Chung YS (2013) The mechanical properties of fly ash-based geopolymer concrete with alkaline activators. Construction and Building Materials 47(2): 409–418.
[45] Doıan M, Bideci A (2016) Effect of Styrene Butadiene Copolymer (SBR) admixture on high strength concrete. Construction and Building Materials 112(4):378-385.
[46] Bouaissi A, Li LY, Al Bakri Abdullah MM, Bui QB (2019) Mechanical properties and microstructure analysis of FA-GGBS-HMNS based geopolymer concrete. Construction and Building Materials 210(12):198–209.
[47] Welter M, Schmücker M, MacKenzie KJD (2015) Evolution of the fibre-matrix interactions in basalt-fibre-reinforced geopolymer-matrix composites after heating. Journal of Ceramic Science and Technology 6(1):17–24.
[48] Al-Rousan R (2019) Behavior of two-way slabs subjected to drop-weight. Magazine of Civil Engineering 90(6):62–71.
[49] Bheemaray, Chittappa HC (2022) Impact analysis of spiral cellular structured hybrid sandwiched panel using ANSYS explicit dynamics. Materials Today: Proceedings, 52(3):1377–1383.
[50] Sohel KMA, Richard Liew JY (2014) Behavior of steel-concrete-steel sandwich slabs subject to impact load. Journal of Constructional Steel Research 100:163–175.
[51] Singh I, Dev N, Pal S, Visalakshi T (2022) Finite element analysis of impact load on reinforced concrete. Lecture Notes in Civil Engineering 203:265–274.
[52] AlAraza HA, Mahmud K (2022) A parametric study of concrete runway pavement layers depression under impact load. Vestnik MGSU 17(9):1206–1217.
[53] Li W, Xu J (2009) Mechanical properties of basalt fiber reinforced geopolymeric concrete under impact loading. Material Science and Engineering A 505(1):178–186.
[54] Annadurai S, Baskar P, Elango KS (2023) Geopolymer concrete reinforced with basalt fibres: An experimental investigation. Materials Today Proceedings. DOI: https://doi.org/10.1016/j.matpr.2023.03.143